The Effect of Slip Boundary Conditions on The Newtonian Die-Swell Flow

Jinan Raad Abdul-Jabbar, Alaa H. Al-Muslimawi*

Department of Mathematics, College of Science, University of Basrah, IRAQ

*Corresponding author E-mail: genan.s712@gmail.com

Doi: 10.29072/basjs.20230101

ARTICLE INFO

Keywords

Die-swell; Finite element methods; Galerkin method; Naiver-Stoke equations; Newtonian fluid.

ABSTRACT

The effect of the slip boundary condition on the Newtonian die-swell free surface issue is the main objective of this study. The major aspect of this article is the determination of the free surface position using the free surface location methodology under the slip boundary condition. A Taylor Galerkin/pressure-correction (TG/PC) finite element method is used to solve this issue numerically. Furthermore, the system of equations that governs such a problem includes a time-dependent momentum equation and a continuity equation for mass conservation. These equations are shown here in an axisymmetric frame with Newtonian flow. The free-surface location is calculated using the Phan-Thien (dh/dt) approach in conjunction with slip boundary impact. This work focuses on the effect of slip boundary condition on swelling ratio for Newtonian representation. The current findings reveal that the slip boundary condition has a considerable impact on the swelling ratio of the fluid, causing a decrease in the fluid swell. Furthermore, the behaviors of solution components are presented.

Received 26 Des 2022; Received in revised form 29 Feb 2023; Accepted 22 Mar 2023, Published 30 Apr 2023

1. Introduction

This paper focus on the effect of slip boundary condition on the swelling ratio of fluid based on the finite element time- stepping scheme. The main point of this study is to merge the free surface location methodology with slip boundary condition. To satisfied this aim a (TG/PC) method is employed, which was successfully executed for various flow conditions. The literature on (TG/PC) method for fluid flows is covered broadly (see for example [1-4]). The specified problems that are taken into account are die-swell flows under the crawling conditions. Where these flows are analyzed at 2D level, symmetrical as well as axial coordinate systems. For creeping die-swell flow many authors used FEM method. Nickell et al. [5] provided the solutions of incompressible jet and free surface flows of Newtonian fluids. Chang et al. [6] studied die-swell for Newtonian and viscoelastic fluids by using Galerkin and collocation methods. Crochet and Keunings [7] went further to display that improvement of mesh, with an increment in the concentricity of elements when singularity, have a significant effect at die-swell calculations. Silliman and Scriven [8] used Galerkin finite element method to see the effect of slip-coefficient boundary on the Newtonian die swell flow. Also, they concerned on their work on the effect of surface tension on the free surface problem. Phan-Thien [9] studied the slip effects on extrudate swell by using a boundary element method, in the planar flows of flexible fluids. Beverly and Tanner [10] also used FEM to study the three-dimensional Newtonian square die, planar die extrusion and L-shaped die extrusion problems. Georgiou et al. [11] employed a singular FEM and integrated singular basis function method to study the die-swell and stick-slip problems. For the purpose of studying the effect of compressibility on the swelling ratio, Georgiou [12] has found a solution to the problem of swelling to the compressible Newtonian flow. Here, a significant influence of compressibility on the swelling is found out. Ngamaramvaranggul and Webster ([13], [14]) Developed a semi-implicit TGPC-FEM for the Newtonian creep free surface flows in the case of incompressible. There, the study focused on the die swell and stick-slip problems for annular, axisymmetric and plane systems. Belblidia et al. [15] use the increasing pressure correction on a time fractional-staged of Taylor-Galerkin to solution both compressible, incompressible inelastic die-swell flows. The authors used various type of inelastic model in their study to see the effect of elasticity on the swelling ratio.

In this study, the problem of extrusion under slip boundary conditions was investigated numerically. Furthermore, this research provides free surface flow issue, which represents a great

challenged in numerical studies. At this context, free-surface predictions approach, named the Phan-Thien (dh/dt) technique has been utilized to address free-surface movement. This method was developed by Phan-Thien [8]. The findings show that there is a significant effect of the slip boundary condition on the level of swelling. In this investigation, the free surface technique is combined with (TG/PC) method (see [16-17]). This combination method is employed to address the die-swell problem. Such problem represents one of the important issues in the fluid application, where recently many studies have been conducted (see [18-20]). Here, the results are given that the slipping conditions lead to reduce in the level of swelling ratio. Furthermore, the behaviors of solution components under slip and no slip conditions are presented as well.

2. Governing equations

The continuity and momentum equations in non-dimensional form for isothermal incompressible flow can be given by:

$$\nabla\cdot\mathbf{u} = 0. \tag{1}$$

$$\frac{\partial u}{\partial t} = \frac{1}{Re}[\nabla.(2\mu d) - Reu.\nabla u - \nabla p]. \tag{2}$$

where, u, p and, μ the velocity, pressure and viscosity of fluid. In addition, d represents the rate of deformation for flows, which can be expressed as

$$\mathrm{d}=\frac{1}{2}(\nabla u + \nabla u^{T}). \tag{3}$$

Further, $Re=\rho\frac{UL_{\circ}}{\mu}$ represents the Reynolds number of the non-dimensional set, where U a characteristic velocity and $L_{\circ}$ is a length-scale.

In the cylindrical component form these eqations may be given as:

Continuity:

$$\frac{1}{r}\frac{\partial r u_r}{\partial r}+\frac{1}{r}\frac{\partial u_\theta}{\partial \theta}+\frac{\partial u_z}{\partial z}=0. \tag{4}$$

Momentum in r -component

$$\frac{\partial u_r}{\partial t}+u_r\frac{\partial u_r}{\partial r}+\frac{u_\theta}{r}\frac{\partial u_r}{\partial \theta}-\frac{u_\theta^2}{r}+u_z\frac{\partial u_r}{\partial z}=-\frac{1}{\rho}\frac{\partial p}{\partial r}+\frac{\mu_s}{\rho}\left(\frac{1}{r}\frac{\partial}{\partial r}\left(r\frac{\partial u_r}{\partial r}\right)-\frac{u_r}{r^2}\right.$$

$$\left.+\frac{1}{r^2}\frac{\partial^2 u_r}{\partial \theta^2}-\frac{2}{r^2}\frac{\partial u_\theta}{\partial \theta}+\frac{\partial^2 u_r}{\partial z^2}\right), \tag{5}$$

Momentum in θ -component

$$\frac{\partial u_\theta}{\partial t}+u_r\frac{\partial u_\theta}{\partial r}+\frac{u_\theta}{r}\frac{\partial u_\theta}{\partial \theta}+\frac{u_r u_\theta}{r}+u_z\frac{\partial u_\theta}{\partial z}=-\frac{1}{r\rho}\frac{\partial p}{\partial \theta}+\frac{\mu_s}{\rho}(\frac{1}{r}\frac{\partial}{\partial r}(r\frac{\partial u_\theta}{\partial r})-\frac{u_\theta}{r^2}$$

$$+\frac{1}{r^2}\frac{\partial^2 u_\theta}{\partial \theta^2}+\frac{2}{r^2}\frac{\partial u_r}{\partial \theta}+\frac{\partial^2 u_\theta}{\partial z^2}), \qquad (6)$$

Momentum in z-component

$$\frac{\partial u_z}{\partial t}+u_r\frac{\partial u_z}{\partial r}+\frac{u_\theta}{r}\frac{\partial u_z}{\partial \theta}+u_z\frac{\partial u_z}{\partial z}=-\frac{1}{\rho}\frac{\partial p}{\partial z}+\frac{\mu_s}{\rho}(\frac{1}{r}\frac{\partial}{\partial r}(r\frac{\partial u_z}{\partial r})+\frac{1}{r^2}\frac{\partial^2 u_z}{\partial \theta^2}+\frac{\partial^2 u_z}{\partial z^2}). \qquad (7)$$

Such that u_r, u_θ and u_z represent the velocity in r direction, θ direction and z direction. (for more details see [21])

3. Numerical scheme

The Taylor-Galerkin/ pressure-correction (TG/PC) scheme was adopted to treat the system of equations (4-7). In summary, the algorithm consists of three stages over each time [t_n , t_{n+1}]. First, at stage 1a, velocity components at half time step $(n+\frac{1}{2})$ can be computed by using the data collected at the *n* time level. Then, in stage 1b, the velocity component u* of the full-time step, is calculated from the data at levels *n* and $(n+\frac{1}{2})$. In stage 2, the pressure difference equation is solved over the full-time step range. Finally, velocity field is recovered at stage 3, to complete the time step cycle. The three stages of the (TG/PC) can be presented matrix-form for each time step as follows:

$$\textbf{Stage 1a}: \quad [\frac{2Re}{\Delta t}M+\frac{1}{2}S](U^{n+\frac{1}{2}}-U^n)=\{-[S+ReN(U)]U+L^Tp\}^n \ , \qquad (8a)$$

$$\textbf{Stage 1b}: \quad [\frac{Re}{\Delta t}M+\frac{1}{2}S](U^*-U^n)=\{-SU+L^Tp\}^n-(Re[N(U)U])^{n+\frac{1}{2}}, \qquad (8b)$$

$$\textbf{Stage 2}: \quad K(P^{n+1}-p^n)-\frac{Re}{\theta\Delta t}LU^* \ , \qquad (8c)$$

$$\textbf{Stage 3}: \quad \frac{Re}{\Delta t}M(U^{n+1}-U^*)=\theta L^T(P^{n+1}-p^n). \qquad (8d)$$

where, **M** is the mass matrix, **S** is the momentum diffusion matrix, **K** is the pressure stiffness matrix, **N(U)** is the convection matrix and *L* is the divergence/ pressure gradient matrix, such that:

$$\boldsymbol{M^{rr}}=\boldsymbol{M^{zz}}=\int_{\Omega^e}\phi\phi^T\,d\Omega,$$

$$[\boldsymbol{N(u_r,u_z)}]=\int_{\Omega^e}(\phi\phi^T u_r\frac{\partial\phi^T}{\partial r}+\phi\phi^T u_z\frac{\partial\phi^T}{\partial z})\,d\Omega,$$

$$\boldsymbol{S^{rr}}=\int_{\Omega^e}\left[2\frac{\partial\phi}{\partial r}\frac{\partial\phi^T}{\partial r}+\frac{2}{r^2}\phi\phi^T+\frac{\partial\phi}{\partial z}\frac{\partial\phi^T}{\partial z}\right]d\Omega, \quad \boldsymbol{S^{zz}}=\int_{\Omega^e}\left[\frac{\partial\phi}{\partial r}\frac{\partial\phi^T}{\partial r}+2\frac{\partial\phi}{\partial z}\frac{\partial\phi^T}{\partial z}\right]d\Omega,$$

$$\boldsymbol{S^{rz}} = (\boldsymbol{S^{zr}})^{\boldsymbol{T}} = \int_{\Omega^e} \left[\frac{\partial \phi}{\partial r} \frac{\partial \phi^T}{\partial z} \right] d\Omega,$$

$$\boldsymbol{\ell_r} = \int_{\Omega^e} \left[\psi \frac{\partial \phi^T}{\partial r} + \frac{1}{r} \psi \phi^T \right] d\Omega\,, \quad \boldsymbol{\ell_z} = \int_{\Omega^e} \left[\psi \frac{\partial \phi^T}{\partial z} \right] d\Omega, \quad \boldsymbol{K} = \int_{\Omega^e} \left[\frac{\partial \psi}{\partial r} \frac{\partial \psi^T}{\partial r} + \frac{\partial \psi}{\partial z} \frac{\partial \psi^T}{\partial z} \right] d\Omega\,.$$

4.Problem specification

4.1 Schematic diagram

The die-swell problem can be identified via two zones of different char- acter, the shear flow inside the die and the free jet flow beyond it. During this study mesh M2-4 was used to extract the numerical solutions (see Figure 1a).

4.2 Boundary conditions and free surface location

A Poiseuille flow (*ps*) is specified at the inlet with $u_z = 2\,(1- r^2)$. As pertaining to the influence of slip boundary conditions on the free surface region, we applied the slip velocity at the die wall by using a function of the slip parameter and velocity gradient, which may be expressed as (see Figure 1b):

$$u_{slip} = B_{s;ip} \frac{\partial u}{\partial r}, \tag{9}$$

where, $\boldsymbol{B_{s;ip}}$ is represented the slip-parameter and $\frac{\partial u}{\partial r}$, is the die wall shear velocity gradient.

The other condition on the free surface is the kinetic state:

$$\frac{\partial h}{\partial t} + u_z \frac{\partial h}{\partial z} - u_r = 0, \tag{10}$$

which, gives the additional equation to calculate the new position of the free surface h(z, t). Thus, a new stage (**stage 4**) adds to the three (TG/PC) stages and takes the following form:

Stage 4: $\frac{1}{\Delta t}(h^{n+1} - h^n) = u_r^n - u_z^n \left(\frac{\partial h}{\partial z}\right)^n$ (11)

(a)

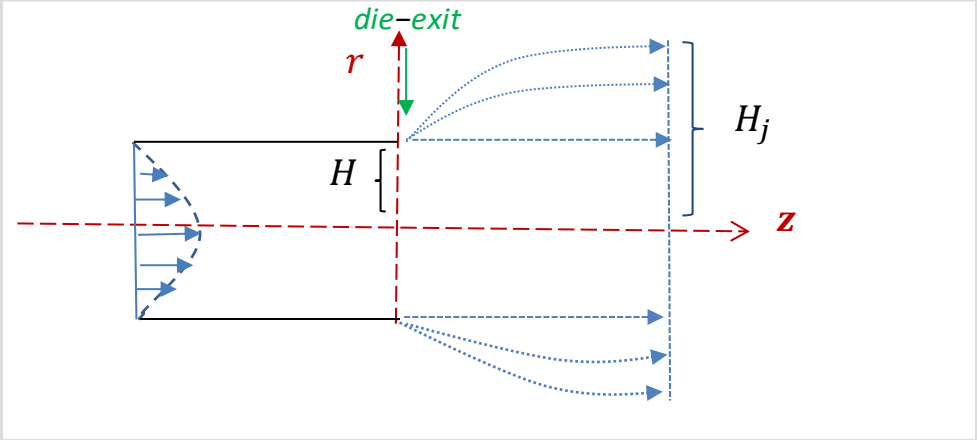

(b)

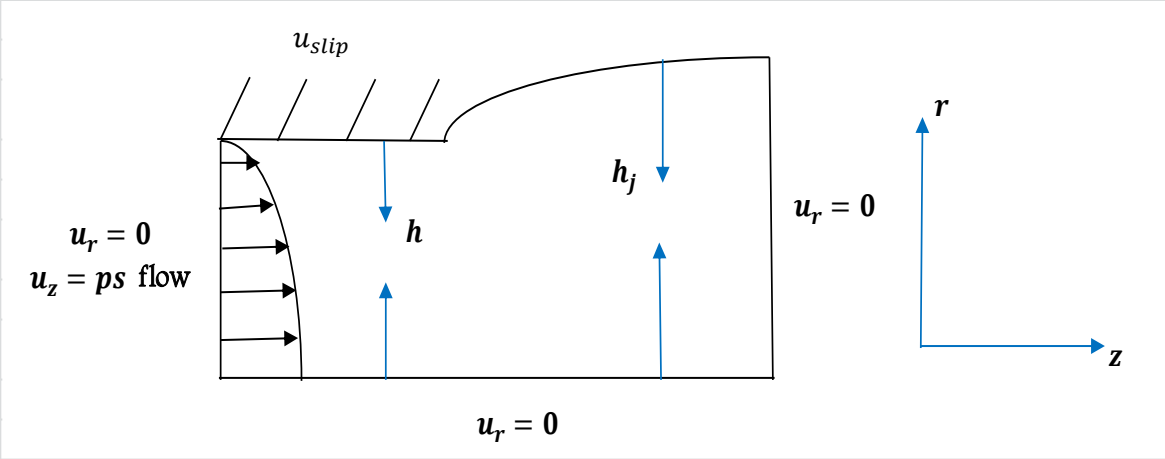

Figure 1: Die-swell geometry

5. Numerical results

Figure 3 illustrates the velocity vector for die section and free surface position with zoomed regions. The finding reflects the effect of free surface condition in the jet zoon, where an initial inlet Poiseuille flow through the die section adjusts to a final plug flow (approximate plug flow is clearly established in the jet section). For more details, the axial velocity u_z is presented in various

regions of die and jet sections {(z=-1, -0.7, -0.3) and (z=1.3, 1.7, 2, 3,4), respectively} (see Figure 4(a,b)). From the profiles one can observe that the behavior of flow is gradually changed from Poiseuille presentation to the plug-flow manner, due to the effect of applying the boundary conditions. In addition, the pressure distribution over the axisymmetric line is displayed in Figure 5, where the high level of pressure is appeared at the entrance of die. In this context, the results show that through the die region a consistent linear decline in pressure is occurred, after which the pressure reduction declines linearly to around zero at the free surface zone.

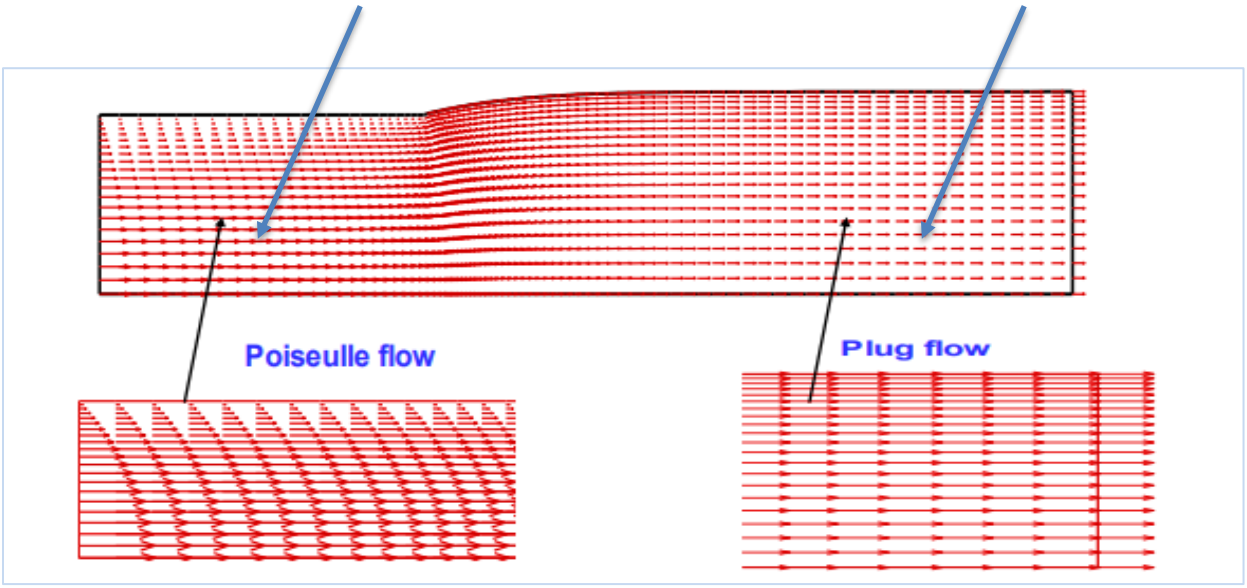

Figure 3: Velocity vector

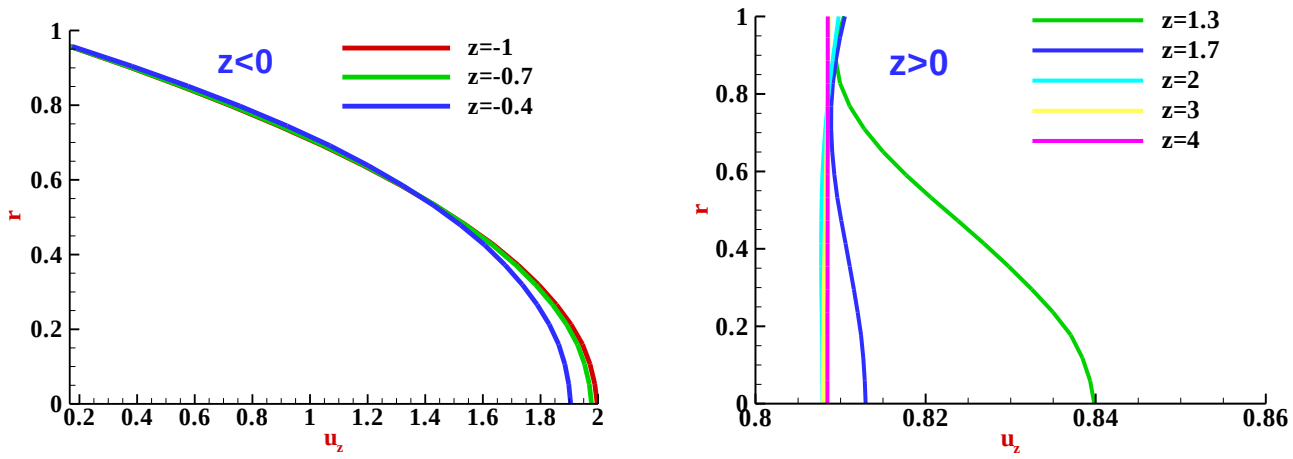

Figure 4: Axial velocity profile (a) die section, (b) jet section

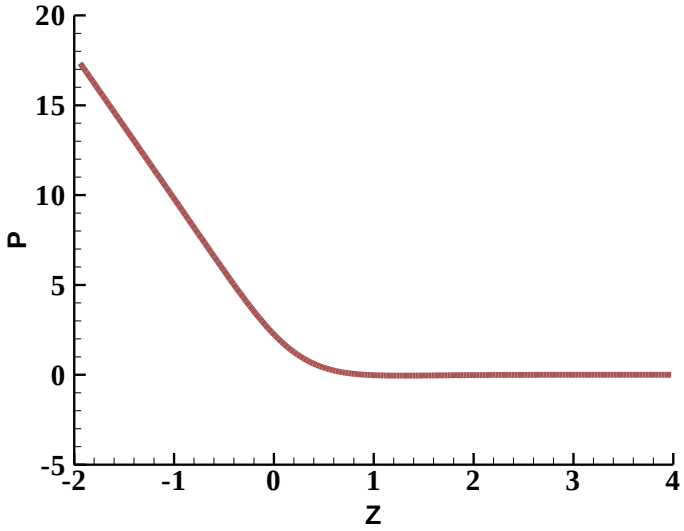

Figure 5: pressure profile on axis of symmetry

More to the above discussion, the influence of slip boundary condition on the solution and swelling ration of fluid is presented as well. In the context, we applied the slip boundary condition on the die wall based on the slip formula (8). Here, this slip equation depends upon slip parameter B_{slip}, which is taken as various level to see the influence of different level of slipping. Firstly, we discussed the impact of slip boundary condition on the level of pressure. Here, comparison in pressure drop along the centerline between the case with slip condition and without slip condition is provided in Figure 6. Note, the influence of slip boundary condition on the level of pressure drop is insignificant with modest rise in the case of no slip condition. Same feature is observed for the velocity (not shown).

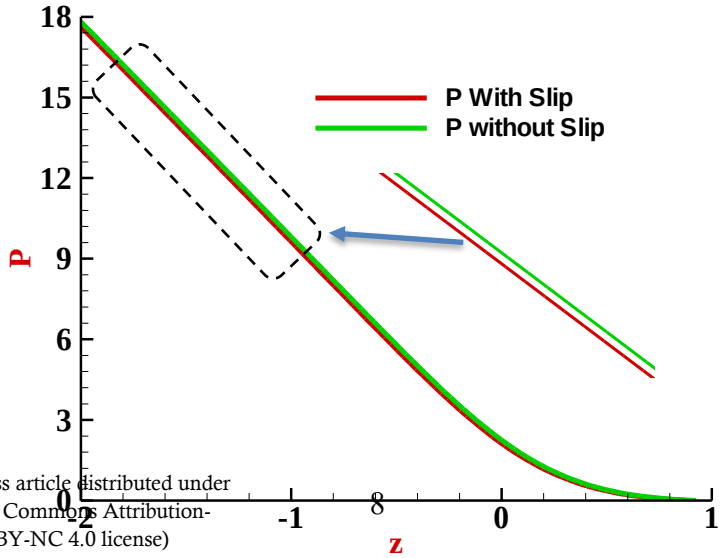

Figure 6: Pressure profile along centerline section

Swelling ratio: The swell ratio is defined as $\chi = \frac{H_j}{H}$, where H and H_j represent the die radius and final extrudate radial, respectively (see Figure 2). The swelling ratio data is plotted in Figure 7 in both cases with slip boundary condition and without slip condition. Finding for swell reveals, the jet swelling with slip boundary condition is lower than that for the case of no slip condition. Moreover, the effect of slip parameter B_{slip} on the swelling ratio is presented in Figure 8, with $\{B_{slip}= 0, 0.03, 0.05, 0.07\}$. from the profiles one can see that the level of swelling ratio is decreased as the level of B_{slip} increased, which reflect the impact of slip wall on extrudate swell.

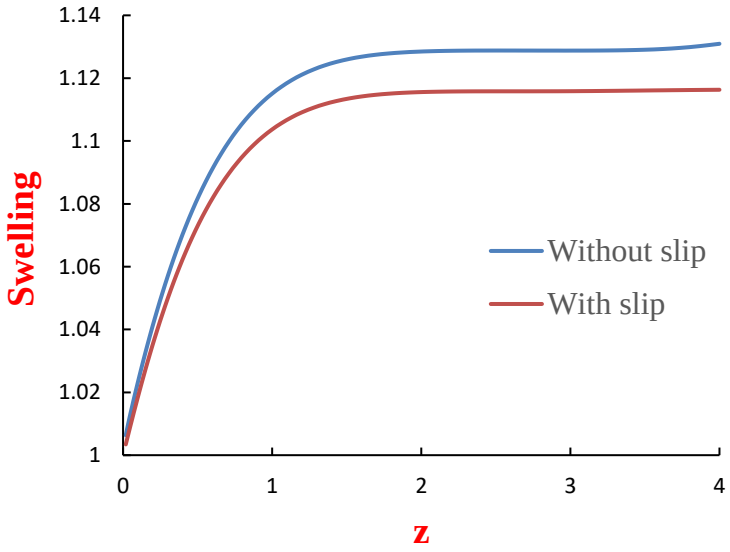

Figure 7: Swell profiles with slip vs without slip

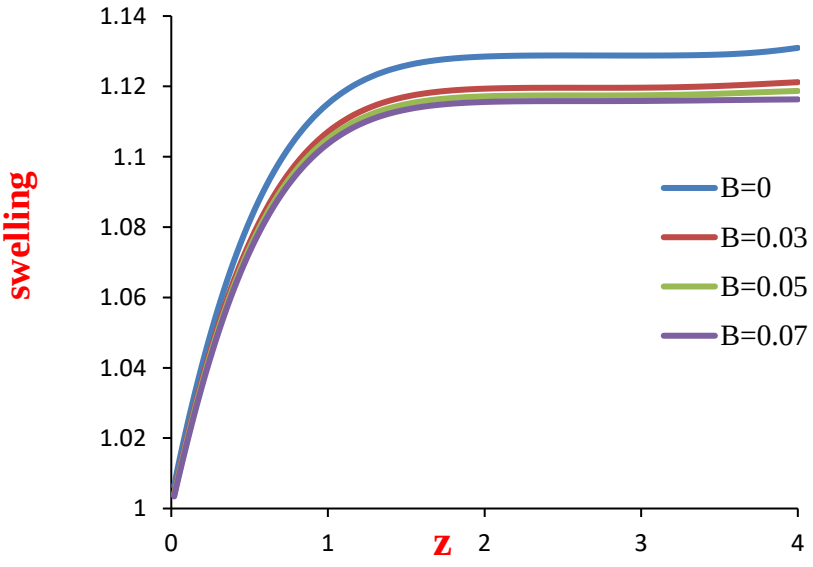

Figure 8: Effect of the slip parameter on swelling ratio

6. Conclusion

In this study, a Taylor Galerkin/pressure-correction (TGPC) finite element scheme was used to presented practical test on the Newtonian die-swell flow that shows the free surface location methodology to determine the free surface position under slip boundary conditions. For this purpose, the calculation of the free surface was carried out using the Phan-Thien (dh/dt) approach in parallel with the slip boundary impact. The behavior of velocity and pressure are investigated throughout this study. Also, the effect of the slip boundary condition on the swelling ratio of the Newtonian representation was shown. In this context, the results that there is a significant effect of the slip boundary condition on the fluid swelling, as it causes a reduce in the fluid swelling.

References

[1] A. Baloch, P. Townsend, M. F. Webster, On two-and three-dimensional expansion flows, Comp. Fluids, 24(1995)863-882, https://doi.org/10.1016/0045-7930(95)00020-D

[2] P. Rameshwaran, P. Townsend, M. F. Webster, Simulation of Particle Setting in Rotating and Non-Rotating Flow of Non-Newtonian Fluids, Int. J. Num. Meth. Fluids, 26 (1998) 851-874, https://doi.org/10.1002/(SICI)1097-0363(19980415)26

[3] A.H. Al-Muslimawi, Theoretical and numerical studies of die swell flow, Korea- Australia Rheology J, 28(2016) 229-236, https://doi.org/10.1007/s13367-016-0023-6

[4] A.H Al-Muslimawi, H.R. Tamaddon-Jahromi, M.F. Webster, Simulation of viscoelastic and viscoelastoplastic die-swell flows, J Non-Newtonian Fluid Mech., 191 (2013) 45-56, https://doi.org/ 10.1016/ j.jnnfm.2012.08.004

[5] R.E Nickell, R.I Tanner, B. Caswell, The Solution of Viscous Incompressible Jet and Free Surface Flows Using Finite-Element Methods, J. Fluid Mech., 65(1974) 189-206, https://doi.org/10.1017/S0022112074001339

[6] P.W Chang, T.W Patten and Finlayson, Collocation and Galerkin Finite Element Methods for Viscoelastic fluid Flow-II, Comp. and Fluids, 17(1979) 285-293, https://doi.org/10.1016/0045-7930(79)90012-4

[7] M.J Crochet, R. Keunings, On Numerical Die Swell Calculation, J. non-Newtonian Fluid Mech., 10 (1982) 85-94, https://doi.org/10.1016/0377-0257(82)85006-4

[8] W.J Silliman, L.E Scriven, Separating Flow Near a Static Contact Line: Slip at a Wall and Shape of a Free Surface, J. Comp. Phys., 34(1980) 287-313, https://doi.org/10.1016/0021-9991(80)90091-1

[9] N. Phan-Thien, Influence of Wall Slip on Extrudate Swell: a Boundary Element Investigation, J. Non-Newtonian Fluid Mech., 26(1988) 327-340, https://doi.org/10.1016/0377-0257(88)80024-7

[10] C.R Beverly, R.I Tanner, Numerical Analysis of Three-Dimensional Newtonian extrudate Swell, Rheol. Acta, 30 (1991) 341-356, https://doi.org/10.1007/BF00404194

[11] G.C Georgiou, L.G Olson, W. WShultz, The integrated singular basis function method for the stick-slip and the die-swell problem, Int. J Numer. Methods Fluids 13 (1991) 1251-1265, https://doi.org/10.1002/fld.1650131005

[12] G.C Georgiou, The compressible Newtonian extrudate swell problem, Int. j. numer. methods fluids 20 (1995) 255-261, https://doi.org/10.1002/fld.1650200305

[13] V. Ngamaramvaranggul, M.F Webster, Computation of free surface flow with a Taylor Galerkin/pressure-correction algorithm, J. Non-Newtonian Fluid Mech. 33 (2000) 993- 1026, https://doi.org/10.1002/1097-0363(20000815)33:7<993::AID-FLD40>3.0.CO;2-A

[14] V. Ngamaramvaranggul, M.F Webster, Viscoelastic simulations of stick-slip and die-swell flows, J. Non-Newtonian Fluid Mech.36(2001) 539-595, https://doi.org/10.1002/fld.145

[15] F. Belblidia, T. Haroon, M.F. Webster, The dynamics of compressible Herschel-Bulkley fluids in die-swell flows, Damage Fracture Mech, Springer, Dordrecht, 2009, 425-43, https://doi.org/10.1007/978-90-481-2669-9_45

[16] V. Ngamaramvaranggul, M.F Webster, Computation of Free Surface Flows with a Taylor-Galerkin/Pressure-correction Algorithm, Int. J. Num. Meth. Fluids, 27(1999), https://doi.org/10.1016/j.cam.2016.06.007

[17] M.S Chandio, M.F Webster, Numerical simulation for reverse roller-coating with free-surfaces, European Congress on Computational Methods in Applied Sciences and Engineering, Swansea, Wales, UK, (2001) 4-7, https://doi.org/10.31642/JoKMC/2018/050203

[18] M.M.A Spanjaards, M.A Hulsen, P.D Anderson, Die shape optimization for extrudate swell using feedback control, J Non-Newtonian Fluid Mech., 293(2021) 1-15, https://doi.org/10.1016/J.JNNFM.2021.104552

[19] M.M.A Spanjaards, M.A Hulsen, P.D Anderson, Transient 3D finite element method for predicting extrudate swell of domains containing sharp edges, J Non-Newtonian Fluid Mech., 270(2019) 79-95, https://doi.org/10.1016/J.JNNFM.2019.07.005

[20] T.M Oyinloye, W.B Yoon, Investigation of flow field, die swelling, and residual stress in 3D printing of surimi paste using the finite element method, IFSET, 78 (2022), https://doi.org/10.1016/j.ifset.2022.103008

[21] B.K Jassim, A H Al-Muslimawi, Numerical analysis of Newtonian flows based on artificial compressibility AC method, J Al-Qadisiyah Comp. Sci. Math., 9(2017) 115-128, https://doi.org/10.29304/jqcm.2017.9.2.303

تأثير شروط حدود الانزلاق على تدفق النفخ المتضخم لنيوتن

جنان رعد عبد الجبار, علاء حسن عبدالله

قسم الرياضيات، كلية العلوم، جامعة البصرة

المستخلص

تهتم هذه الدراسة بتأثير حالة حدود الانزلاق على مشكلة السطح الخالي من الانتفاخ النيوتوني. عمليًا، يمثل تحديد موضع السطح الحر استنادًا إلى منهجية موقع السطح الحر في ظل حالة حدود الانزلاق السمة الرئيسية في هذه الورقة. يتم التعامل مع هذه المشكلة عدديًا باستخدام طريقة تايلور جاليركين / تصحيح الضغط (TG / PC). بالإضافة إلى ذلك، يتكون نظام المعادلات التي تحكم هذه المشكلة من معادلة الزخم المعتمدة على الوقت ومعادلة الاستمرارية للحفاظ على الكتلة. تم تقديم هذه المعادلات هنا في إطار محور متماثل مع تدفق نيوتن. يتم حساب موضع السطح الحر باستخدام طريقة Phan-Thien (dh/ dt) بالتوازي مع تأثير حد الانزلاق. بشكل أساسي، توفر هذه الدراسة تأثير حالة حد الانزلاق على نسبة التورم للتمثيل النيوتوني. تظهر النتائج الحالية أن هناك تأثيرًا كبيرًا من حالة حدود الانزلاق على نسبة التورم في السائل، حيث يتسبب في تقليل تضخم السائل. علاوة على ذلك ، يتم عرض سلوكيات مكونات الحل أيضًا.